Pergamon

Journal of Structural Geology, Vol. 17, No. 4, pp. 575 to 588, 1995

0191-8141/95 $9.50+0.00

0191-8141(94)00077-8

Geometric and kinematic models for detachment folds with fixed and variable detachment depths

THOMAS X. HOMZA and WESLEY K. WALLACE

Tectonics and Sedimentation Research Group, Department of Geology & Geophysics and Geophysical Institute, University of Alaska Fairbanks, Fairbanks, AK 99775, U.S.A.

(*Received* 9 *October* 1993; *accepted in revised form* 31 *May* 1994)

Abstract—Detachment folds are defined by competent rock units and are cored by incompetent units deformed internally above a detachment horizon. We have developed two geometric models to constrain possible geometries and kinematic paths for ideal detachment folds. The models each independently relate fold geometry to shortening and to detachment depth. Model assumptions include plane-strain, constant competent bed-length, constant cross-sectional area, chevron fold geometry, and no bed-parallel shear outside the fold. Detachment depth is constant in one model but may vary in the other, thus allowing evaluation of the implications for fold geometry and kinematics of fixed vs variable detachment depth.

Detachment folds formed above a detachment unit of constant thickness (constant detachment depth) must be initially symmetrical and cannot grow with fixed hinges (fixed arc-length) or a self-similar geometry. Detachment folds formed above a detachment unit of variable thickness (variable detachment depth) must also be initially symmetrical, but any one fold geometry can have a range of possible initial and final detachment depths. Kinematic paths for folds with fixed hinges (fixed arc-lengths), migrating hinges (variable arc-lengths), and self-similar geometries are all possible if detachment depth varies. The change in detachment depth during deformation can be determined using the variable detachment depth model if either initial or final detachment depth is known.

The models demonstrate a wider range of variability in the geometry and kinematics of ideal detachment folds, particularly for the variable-depth model, than is the case for ideal fault-bend and fault-propagation folds. This variability limits the usefulness of simple geometric models for reconstructing the geometry of natural detachment folds. Balancing cross-sections over a sufficient area and evaluating strain may compensate for these limitations.

INTRODUCTION

Three major types of thrust-related folds have been recognized in fold-and-thrust belts (Jamison 1987) (Fig. 1): fault-bend folds (Suppe 1983, Jamison 1987), fault-propagation folds (Jamison 1987, Mitra 1990, Suppe & Medwedeff 1990), and detachment (or décollement) folds (Dahlstrom 1969, 1970, 1990, Jamison 1987, Mitra & Namson 1989, Mitra 1992). Detailed descriptions have been given of the geometry and kinematics of fault-bend folds (Suppe 1983) and fault-propagation folds (Suppe & Medwedeff 1990, Mitra 1990). However, a comparable treatment of the geometry and kinematics of detachment folds is lacking in the literature to date. Here we present two geometric models for detachment folds that provide a framework for describing and constraining their kinematic evolution.

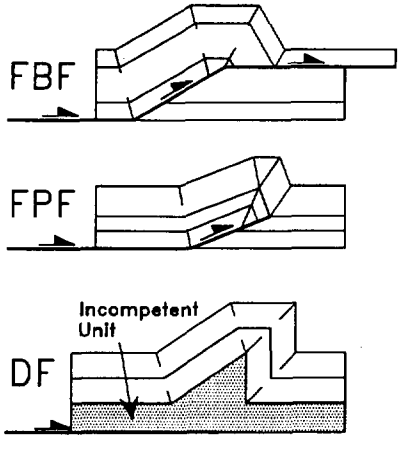

Fig. 1. Three major types of thrust-related folds in fold-and-thrust belts: fault-bend fold (FBF), fault-propagation fold (FPF), and detachment fold (DF).

Alternating mechanically competent and incompetent rock units constitute the stratigraphy in most fold-and-thrust belts, and folds in relatively competent units with internally deformed weaker rock in their cores are common. We consider a detachment fold to be a fold in a relatively competent rock unit that is cored by internally deformed less competent rock that is separated from another competent unit by a detachment horizon or décollement. Detachment folds may be bounded by detachment horizons above, below, or both. Many detachment folds may be buckle folds, but many buckle folds are not detachment folds because they are not bounded by a detachment horizon.

Geometries that we consider characteristic of detach-

ment folds are widespread in nature and have been recognized since the 19th century [see Willis & Willis (1934) for a review]. However, because of the lack of a clear and widely used definition of the term 'detachment fold', many folds with appropriate geometries have not been explicitly identified as detachment folds. Consequently, it is difficult to use published information to assess the full range of detachment fold geometries that exist in nature. Another difficulty in documenting the geometry and kinematics of detachment folds is that few geometric constraints can be imposed upon deforming incompetent rocks, thus requiring the use of simplifying assumptions about fold geometry and kinematics.

Here, we describe quantitatively the implications of one fundamental assumption that is commonly made about detachment folds: that detachment depth remains constant during folding. We have chosen to focus on this assumption because its validity and quantitative implications have not been as thoroughly explored as others and because variability of detachment depth due to thinning or thickening of the incompetent unit is quite plausible in detachment folds (Wiltschko & Chapple 1977, Davis & Engelder 1985).

We have developed two simple, theoretical, quantitative models for the geometry of detachment folds based on the law of conservation of volume (Goguel 1962, Dahlstrom 1969, 1990, Mitra & Namson 1989). The first model is for detachment folds formed above a detachment unit of constant thickness (constant detachment depth model) and the second is for detachment folds formed above a detachment unit that changes thickness during folding (variable detachment depth model).

We do not assume that these models directly represent natural folds. Rather, they provide idealized standards against which natural folds can easily be compared. Such comparisons can be made using easily obtained geometric measurements, rather than values related to fold mechanics or dynamics that are far more difficult to constrain. The explicit assumptions incorporated in the models isolate the variables that may influence fold geometry and kinematics.

CONSERVATION OF LINE-LENGTH AND AREA IN DETACHMENT FOLDS

The concepts of conservation of bed length and cross-sectional area (e.g. Goguel 1962, Hossack 1979, Geiser 1988) are widely known and applied to the balancing of structural cross-sections in foreland fold-and-thrust belts that have been deformed in plane-strain at relatively low temperatures and pressures (Woodward *et al.* 1985, 1989). Our detachment fold models, like those of Dahlstrom (1969, 1990), Jamison (1987) and Mitra & Namson (1989), rely fundamentally on these two concepts: (1) that competent units form parallel folds by flexural slip with cross-sectional bed length conserved during deformation, and (2) that cross-sectional area is conserved during deformation.

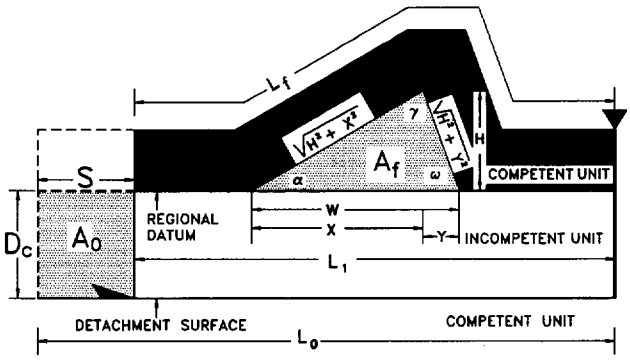

Fig. 2. Geometric basis for the fixed detachment depth model. As the incompetent unit is displaced and shortened, conservation of cross-sectional area requires that the displaced area (A_0) equal the uplifted area (A_f). Conservation of line-length requires the contact between competent and incompetent units to retain its original length ($L_0 = L_f$). See text for explanation of other variables.

Conservation of bed length can be expressed as the 'line-length constraint':

$$S = L_f - L_1 \quad (1)$$

where S is shortening, L_f is the arc-length of a reference bed after folding and L_1 is the horizontal component of the folded length of the reference bed (Fig. 2).

Conservation of cross-sectional area can be expressed as 'the area constraint':

$$SD_c = A_f \quad (2)$$

where D_c is constant detachment depth and A_f is the area of the incompetent unit uplifted above its undeformed regional base level as a result of shortening (Fig. 2).

In an ideal detachment fold, bed length is conserved in the parallel-folded competent unit that defines the fold but not in the detached, incompetent unit that cores the fold. An incompetent unit, such as salt or shale, does not form parallel folds at the scale of the entire unit, but rather deforms internally by some combination of folding, faulting and penetrative strain. Thus, these units tend to thicken during deformation so that unit length apparently decreases. Although line-length balancing is invalid for incompetent rocks, conservation of cross-sectional area is still assumed to apply. The contact between the competent unit and the adjacent incompetent unit defines the original length of that incompetent unit. Thus, equations (1) and (2) can be combined as 'the equal area equation':

$$D_c = A_f/(L_f - L_1). \quad (3)$$

This relationship has been accepted and widely used in various forms with differing degrees of success since Chamberlin (1910) first used it to estimate detachment depths beneath Appalachian folds (Bucher 1933, Goguel 1962, Laubscher 1962, Dahlstrom 1969, Jamison 1987, Mitra & Namson 1989, Thompson 1989, Mitra 1992, Epard & Groshong 1993). Jamison (1987) used this relationship to establish the range of possible detachment fold geometries for different ratios of fold height to detachment depth. He also relaxed the con-

straint of constant bed-length in the competent unit to explore the geometric consequences of forelimb thickening and thinning. Mitra & Namson (1989) used the relationship to develop a model for symmetrical detachment folds. In their model, additional variations in fold geometry were attained by allowing vertical variations in bed-parallel shear. Epard & Groshong (1993) eliminated the assumption of constant bed-length in their use of the equal-area method to determine the required constant detachment depth beneath detachment folds. In each of the references above, the equal-area method has been used assuming a constant detachment depth. The models presented below explore the implications of this assumption and the consequences of relaxing it.

THE MODELS

We present two simple, idealized geometric models for detachment folds that are based on relating the line-length and area constraints. The only assumptions about mechanical behavior are that an upper competent unit deforms by parallel folding and a lower incompetent unit deforms internally. These mechanical concepts of competence vs incompetence, which are difficult to quantify practically, are represented in the models by their geometric equivalents, fixed vs variable thickness and length, which are easy to observe and measure. The models assume a simple triangular fold form common among natural detachment folds (e.g. Jamison 1987, Wallace & Hanks 1990, Homza 1992, Wallace 1993), but the equations presented below can be modified to accommodate more complicated geometries. An ideal parallel kink-fold geometry is used for the competent unit, with no thinning or thickening of limbs, and plane strain is assumed, so there is no change in cross-sectional area during shortening. The models consider only single folds and so apply only to those multi-fold systems in which adjacent detachment folds do not overlap. Bed-parallel shear is assumed to be absent outside of the detachment fold in both the competent and incompetent units and the detachment surface is assumed to parallel the regional datum defined by the fold (Fig. 2). Thus, the major geometric constraints for both models are simply that the competent unit must conserve line-length and the incompetent unit must conserve area. The sole difference between the two models is the assumption of constant depth in the first model but not in the second.

Constant detachment depth model

The first model represents detachment folds formed above a detachment horizon that maintains a constant depth (thickness) during folding (Fig. 2). The power of this model lies in the fact that both detachment depth and shortening can be determined independently given only the geometry of the detachment fold. This geometry can be expressed uniquely in terms of any three of the following variables, including at least one linear dimension: interlimb angle (γ), backlimb dip (α), forelimb dip (ω), wavelength (W), and height (H) (where γ and $\omega < 180°$ and $\alpha < 90°$). The equations derived here are expressed in terms of γ, α, and H, and all angles are expressed in degrees.

Using the appropriate variables above, the area constraint (equation 2) can be expressed as:

$$D_c = WH/2S. \tag{4}$$

Similarly, the line-length constraint (equation 1) can be expressed as:

$$S = \sqrt{(H^2 + X^2)} + \sqrt{(H^2 + Y^2)} - W \tag{5}$$

where X and Y are the bases of two separate right triangles that together describe the form of the fold. The following relationships are also implicit from Fig. 2:

$$W = X + Y \tag{6}$$

$$\alpha + \gamma + \omega = 180° \tag{7}$$

$$Y = H \cot \omega \tag{8}$$

$$X = H \cot \alpha. \tag{9}$$

Substituting equations (8) and (9) into equation (6), and expressing ω as $(180 - \gamma - \alpha)$ yields:

$$W = H\{\cot (180 - \gamma - \alpha) + \cot \alpha\}. \tag{10}$$

To solve for the shortening that is geometrically required to uplift the area bounded by the triangular fold, substitute equations (8), (9) and (10) into equation (5), again expressing ω as $(180 - \gamma - \alpha)$, and rearrange such that:

$$S = \sqrt{\{H^2 + (H \cot \alpha)^2\}} + \sqrt{[H^2 + \{H \cot (180 - \gamma - \alpha)\}^2]} - H\{\cot (180 - \gamma - \alpha) + \cot \alpha\}. \tag{11}$$

To solve for the fixed detachment depth (D_c) that is geometrically required to uplift the area bounded by the triangular fold, substitute equations (10) and (11) into equation (4) and rearrange such that:

$$D_c = H^2\{\cot (180 - \gamma - \alpha) + \cot \alpha\}/2(\sqrt{\{H^2 + (H \cot \alpha)^2\}} + \sqrt{[H^2 + \{H \cot (180 - \gamma - \alpha)\}^2]} - H\{\cot (180 - \gamma - \alpha) + \cot \alpha\}). \tag{12}$$

Notice that the detachment depth calculation is based on the area constraint (equation 2), whereas the shortening calculation is based on the line-length constraint (equation 1), and that each is expressed entirely in terms of fold geometry (i.e. γ, α and H). Equations (10), (11) and (12) can be solved in terms of the forelimb dip, ω, simply by substituting ω for α (also note that the expression $(180 - \gamma - \alpha)$ is left in expanded form so it can easily be replaced by ω, since $\omega = (180 - \gamma - \alpha)$). Solving equations (11) or (12) in terms of W rather than

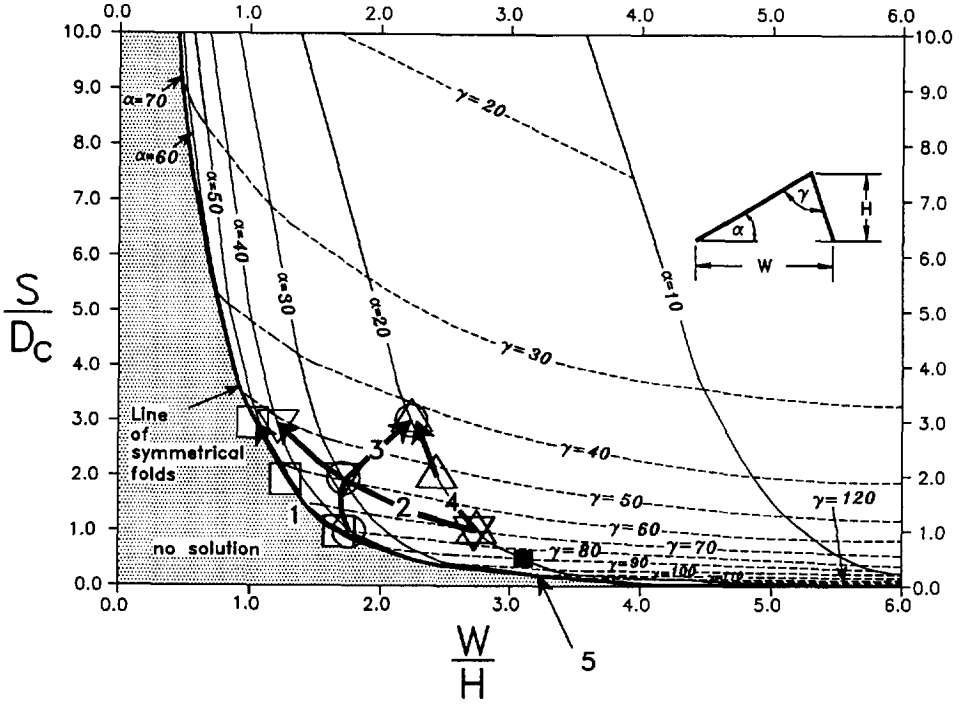

Fig. 3. The constant detachment depth diagram. See text for discussion. Any point on the graph outside of the 'no solution' area defines one and only one triangular fold geometry. No trigonometric solutions exist for the shaded region. See Figs. 4 and 5 for explanation of symbols and numbered kinematic paths.

H, or in terms of α and ω rather than γ, requires different sequences of substitution that are not presented here. Equation (12) is analogous to equation (21) of Jamison (1987).

In conclusion, if any three of the variables γ, α, ω, H, W, S, or D_c are known, including at least one linear dimension, the others can be determined, specifying a unique fold geometry and size.

The constant-depth diagram. The relationship between shortening and fold geometry must be considered in order to determine possible kinematic paths for detachment folds. This relationship was considered qualitatively by Dahlstrom (1990), but was not directly addressed by either Jamison (1987) or Mitra & Namson (1989). The fold geometries predicted by our model can be plotted as a function of shortening/constant detachment depth (S/D_c) vs wavelength/height (W/H), with interlimb angle (γ) and backlimb dip (α) varying according to equations (11) and (12) (Fig. 3). Every point on this 'constant-depth diagram' describes one and only one fold form, although the size of each form varies as a function of shortening and detachment depth. Length ratios are used on this plot instead of absolute lengths in order to represent the large number of variables on a single plot for fold geometry, which can be used to trace kinematic paths.

Since the kinematic evolution of a fold is controlled by increasing shortening, this plot constrains the possible kinematic paths that an ideal detachment fold may follow. The kinematic path must be continuous from the inception to the final form of the fold. Since the detachment depth is held constant, any fold must follow a path with an increasing value of S/D_c as shortening increases.

Implications of the constant-depth diagram for the kinematic evolution of ideal detachment folds. The lower boundary of the field of possible fold geometries in Fig. 3 is the 'line of symmetrical folds', which is asymptotic to $S/D_c = 0$. In order for the graphical plot of successive geometries of an evolving fold to proceed from the $S/D_c = 0$ line to the line of symmetrical folds, the fold must either: (1) nucleate at $W/H = \infty$; or (2) nucleate with a geometry corresponding to the upper boundary of a finite field for which our equations have no solutions (shaded area on Fig. 3). Thus, natural detachment folds could: (1) nucleate with a very high W/H and initially symmetrical geometries; or (2) nucleate after a finite amount of shortening was accommodated by mechanisms other than folding (see Biot 1961, Dixon & Tirrul 1991 and Abbassi & Mancktelow 1992 for additional discussion and references about fold nucleation). In either case, the relative position of the line of symmetrical folds at the base of the range of permissible shapes implies that the initial form of an *ideal* detachment fold is symmetrical.

Folds may become asymmetrical with increasing shortening depending on whether or not the kinematic path follows the line of symmetrical folds. If detachment depth is fixed, equations (11) and (12) require that at least two limb angles change with increasing shortening (Figs. 3 and 4). Thus, growth of a self-similar, fixed limb-dip geometry is not possible with a fixed detachment depth (Figs. 3 and 5a). If detachment depth is fixed, the

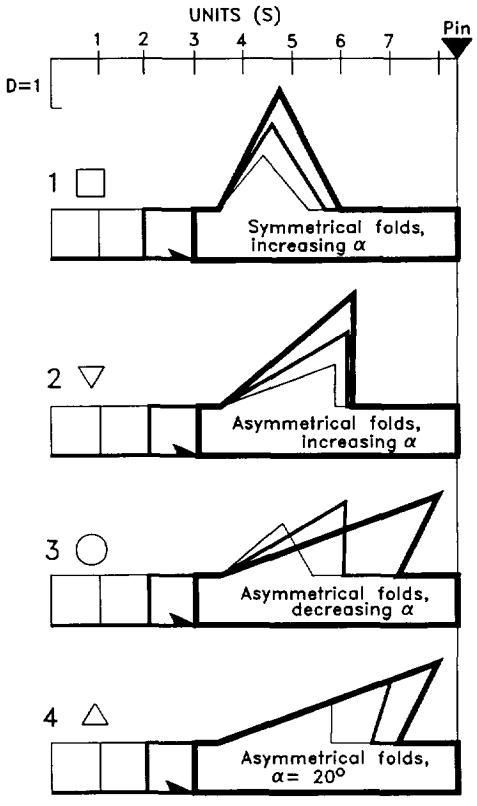

Fig. 4. Kinematic evolutions of fold geometries compatible with the constant detachment depth model. Progressively thicker lines indicate successive steps in fold evolution with increasing shortening above a constant detachment depth. Numbered lines on Fig. 3 represent the kinematic paths for each fold sequence, and symbols mark points describing the geometry of the successive steps in the evolution of each fold.

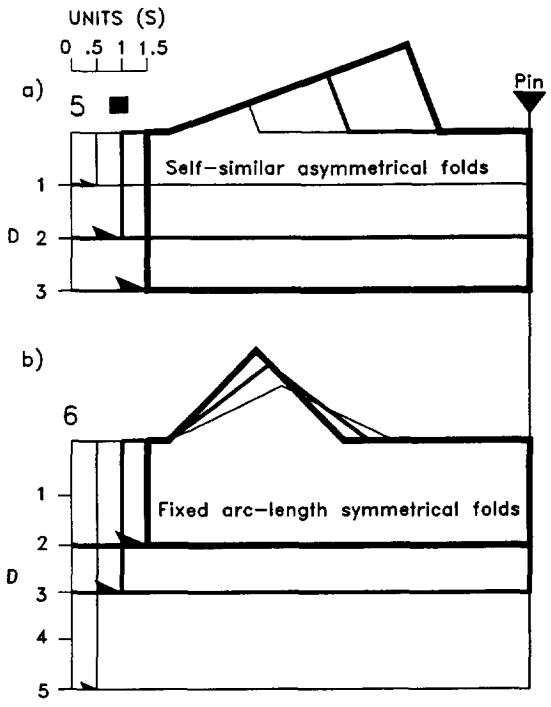

Fig. 5. Successive fold geometries in sequences 5 and 6 are systematically related, but are kinematically impossible within the bounds of the constant detachment depth model because they require variation in detachment depth. Progressively thicker lines indicate successive steps in fold evolution with increasing shortening. Sequence 5 plots as a point on Fig. 3, whereas sequence 6 is omitted for clarity.

equations also require an increase in total limb length as shortening increases so that fixed arc-length buckle folds are not possible (Dahlstrom 1990) (Fig. 5b).

Variable detachment depth model

The variable detachment depth model (Fig. 6) permits a wider range of geometries and kinematic paths than does the constant depth model. In this model, the fold area depends simply on fold geometry and is independent of detachment depth. We define D_o as the undeformed thickness of the incompetent unit (original depth), D_f as the final thickness of the incompetent unit beneath the fold (final depth), and ΔD as the variation in incompetent unit thickness during deformation (Fig. 6) such that:

$$\Delta D = D_f - D_o \tag{13}$$

$$A_o + A_{D_o} = A_f + A_{D_o} + A_{\Delta D} \tag{14}$$

$$A_o = SD_o \tag{15}$$

$$A_{D_o} = W(D_o) \tag{16}$$

$$A_f = WH/2 \tag{17}$$

and the 'area differential'

$$A_{\Delta D} = W(\Delta D). \tag{18}$$

These equations can be combined to yield:

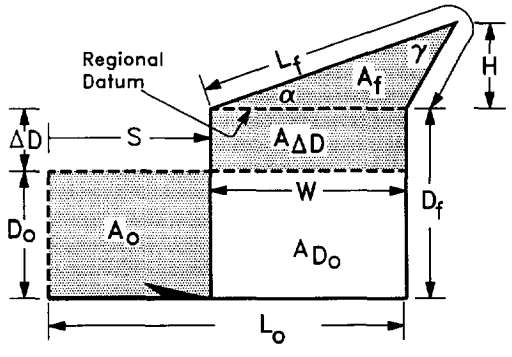

Fig. 6. Geometric basis for the variable detachment depth model. As the incompetent unit is displaced and shortened, conservation of cross-sectional area requires that the displaced area (A_o) equal the uplifted area (A_f) plus the area differential ($A_{\Delta D}$). Conservation of line-length requires the contact between competent and incompetent units to retain its original length ($L_o = L_f$). See text for explanation of other variables.

$$D_f = D_o S/W + D_o - H/2 \tag{19}$$

or:

$$D_f/D_o = S/W + 1 - H/2D_o. \tag{20}$$

Given a specific fold geometry, either the final detachment depth beneath the fold (D_f) or the original detachment depth (D_o) can be determined if the other is known. D_o is invariant, since it represents the undeformed thickness of the incompetent unit. We assume D_o is known, as would be the case where the undeformed stratigraphic thickness of the incompetent unit can be determined outside the fold. However, we stress

that if D_f is known, D_o can be determined by modifying the equations.

The area differential. The area differential ($A_{\Delta D}$ in Fig. 6) represents the difference between the displaced area ($A_o = SD_o$) and the cross-sectional area of the fold (A_f). The area differential can be either positive or negative depending on whether the fold area is smaller or larger, respectively, than the displaced area. A positive area differential indicates a final detachment depth that is greater than the original detachment depth, perhaps due to layer-parallel thickening in the incompetent unit (e.g. Fig. 6). Such structural thickening beneath folds is a common feature in physical models of folds (e.g. Dixon & Tirrul 1991) and in natural detachment folds (e.g. Wallace 1993, Homza 1992, 1993). A negative area differential indicates an original depth that is greater than the final depth, perhaps due to vertical transport of excess material from directly beneath the fold into the fold. Such thinning during folding is also a common feature both in physical models of folds and in natural folds, especially in the early stages of fixed arc-length folding when W/H is large (Wiltschko & Chapple 1977, Dixon & Tirrul 1991, Dixon & Liu 1992). In order to establish a quantitative relationship between the undeformed and shortened states, it is necessary to define boundaries on the area within which the incompetent unit may move during deformation. In this model, material is arbitrarily assumed not to be transported through the lines perpendicular to the detachment surface and connected to the synformal hinges bounding the fold, although the thickness of the incompetent unit directly beneath the synformal hinges may vary. In other words, all of the material in and beneath the antiform is assumed to have originated in the area bounded by the synformal hinges and the geometry outside of the synforms is not considered. The regional datum as defined by the synformal hinges at the base of the competent unit is also assumed to remain parallel to the detachment surface.

The variable-depth diagram. Detachment folds formed above an incompetent layer that changed thickness during deformation, such that $D_f \neq D_o$, can be plotted on a variable-depth diagram (Fig. 7). The diagram consists of two linked graphs: the upper graph is analogous to the constant-depth diagram since it is used to plot fold geometries and every point on the graph represents one and only one fold form; the lower graph has the same X-axis as the upper graph and is used to determine the variation in detachment depth. As with the constant-depth plot, length ratios are used on the upper graph in order to allow the large number of variables to be shown on a single plot for fold geometry. For any fold geometry, only one linear dimension is needed to calculate the others using the equations above. The lower graph is required to accommodate the additional variable, detachment depth. It is the plot of a straight line, the 'depth line', for which the slope is one and $(1 - H/2D_o)$ is the Y-intercept (equation 20). The

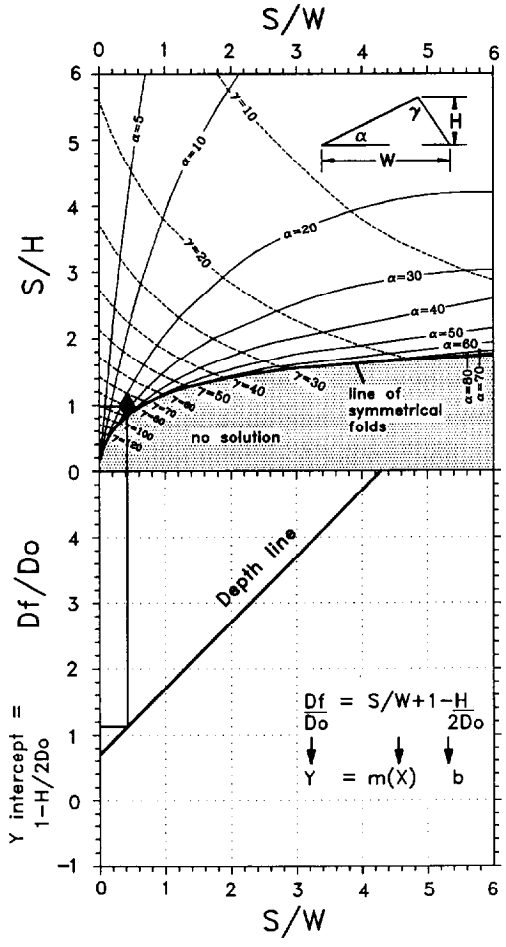

Fig. 7. The variable detachment depth diagram. See text for discussion. D_f/D_o = depth ratio. Any point on the upper graph outside of the 'no solution' area defines one and only one triangular fold geometry. Detachment depth is determined using D_f/D_o, which is the Y-value of the point of intersection of S/W and the appropriate depth line. The fold in Fig. 14 is plotted on this diagram.

position of this line on the Y-axis is determined, therefore, by H and D_o. However, since D_o remains constant, any shift of the depth line on the Y-axis along a kinematic path is a function only of variation in H (Figs. 8 and 9).

Determining the detachment depth for a given detachment fold with a known D_o requires several steps (Figs. 8 and 9). First, the fold geometry must be plotted as a point on the upper graph. Second, a depth line with the appropriate Y-intercept is constructed on the lower graph. Finally, a vertical line, representing S/W of the fold, is drawn to link the point defining the geometry with the depth line. The S/W line and the depth line intersect on the lower graph at a point which defines the D_f/D_o value (Y-value) for the given geometry and given D_o. Thus, D_f can easily be calculated since D_o and D_f/D_o are now both known. It is important to note that multiple depth lines may be needed in order to trace the geometric evolution of a fold along a particular kinematic path since the evolution may involve changes in the value of H (e.g. Fig. 9).

Implications of the variable-depth diagram for the kinematic evolution of ideal detachment folds. A fold

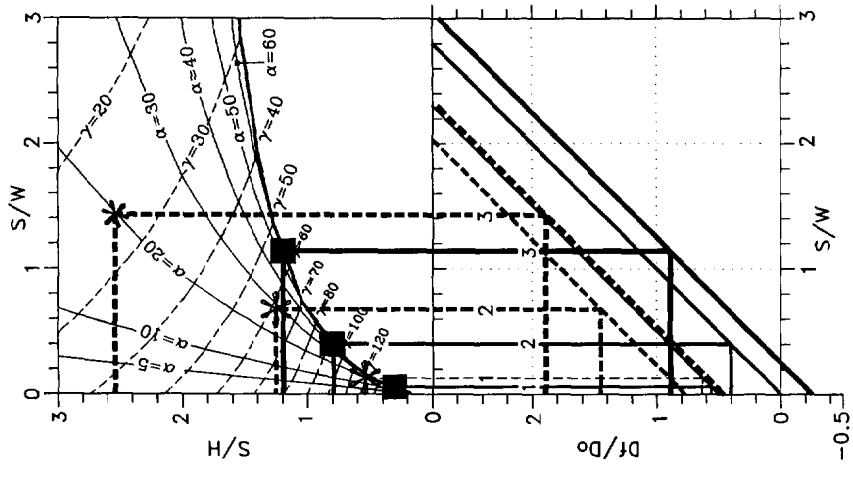

Fig. 9. Graphical plot of the two fold sequences in Fig. 8 on the variable-depth diagram. The line thicknesses and line-types correspond to the folds in Fig. 8. The plot of fold sequence 8(a) (■) moves up the line of symmetrical folds and the correlative Df/Do values show a decrease, then an increase, although Df is less than Do for the geometries shown. Df/Do decreases then increases for fold sequence 8(b) (*) with the depth for the first fold being less than Do, and greater than Do for the later folds shown.

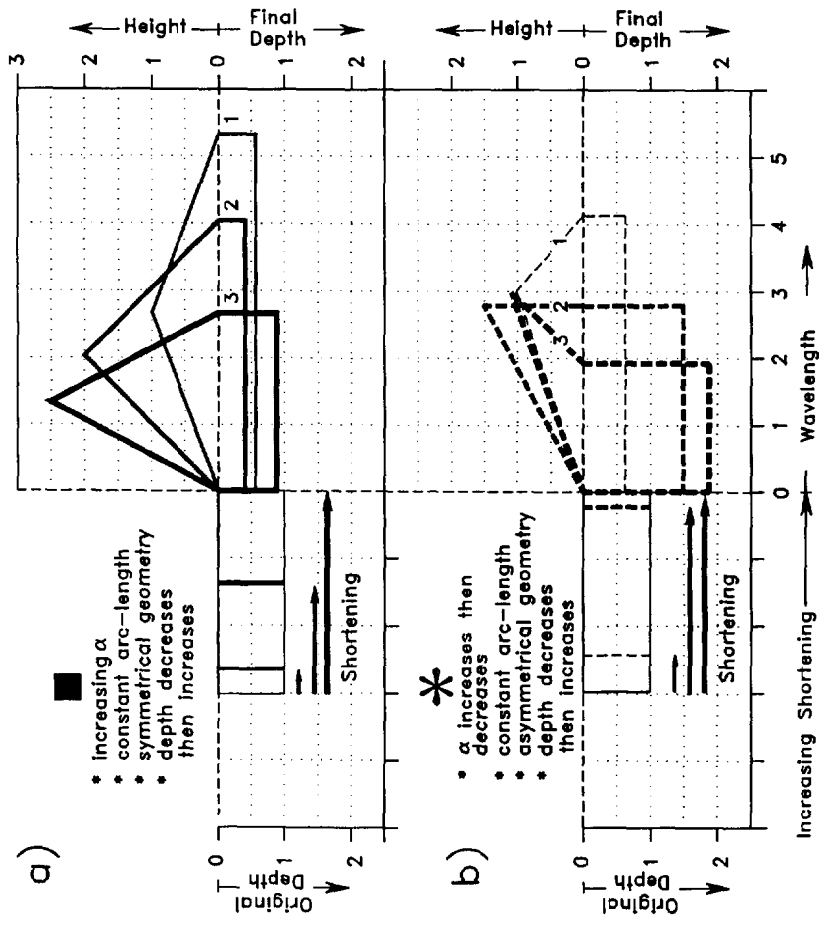

Fig. 8. Kinematic evolution of (a) symmetrical, and (b) asymmetrical fixed-hinge (fixed arc-length) folds. The line weight and shortening increase for folds 1 through 3. The original depth is fixed for each sequence, but depth, height, and wavelength vary with increasing shortening. The symbols and line-type (i.e. solid vs dashed) correspond to the graphical plot of these sequences on Fig. 9. The stratigraphic position of the detachment surface remains constant whereas the thickness of the incompetent unit (and hence detachment depth) varies. To simplify geometric comparison in these figures, the regional datum is used as a fixed reference frame although in natural folds it is more likely that the detachment surface would remain fixed and the elevation of the regional datum would change with incompetent unit thickness.

evolves incrementally as shortening increases. Its kinematic path must be a continuous curve for which values of either S/H or S/W increase. Either ratio may decrease. If both ratios decrease together, however, then shortening decreases, which is not a viable kinematic path. All other paths are considered geometrically viable, although some may be geologically implausible. The line of symmetrical folds on this diagram is asymptotic to $S/H = 0$, suggesting identical geometric implications to those described above for fold nucleation with a fixed detachment depth. An infinite array of geometrically possible kinematic paths can be plotted on the variable-depth diagram. Examples of kinematic paths for fixed arc-length (Figs. 8 and 9), constant-depth (Figs. 10a and 11), and self-similar (Figs. 10b and 11) folds are shown here to illustrate specific implications of variable detachment depth for fold evolution.

Fixed arc-length growth requires a path of first decreasing, then increasing depth, as has been noted by Wiltschko & Chapple (1977) and Dahlstrom (1990) (Figs. 8 and 9). On the variable-depth diagram, a kinematic path for geometries with a constant detachment depth requires that the S/W line and the depth lines intersect at $D_f/D_o = 1$ for every increment of growth (Figs. 10a and 11). Self-similar geometric growth requires a decrease in detachment depth as shortening increases in order for the geometry to balance (Figs. 10b and 11).

THE KINEMATICS OF DETACHMENT FOLDS: FIXED OR MIGRATING HINGES?

Empirical observations and mechanical considerations suggest that buckle folds in a competent layer bounded by incompetent material nucleate with an arc length that is a function of rheology and competent layer thickness, and retain a constant arc length and hence fixed hinges as shortening increases and the fold grows (de Sitter 1956, Biot 1961, Currie *et al.* 1962, Ramberg 1964, Ramsay 1967, 1974, Johnson 1977, Abassi & Mancktelow 1992, Fischer *et al.* 1992, Mancktelow & Abassi 1992) (Fig. 12a). Mitchell & Woodward (1988) assumed that detachment folds form by this fixed arc-length buckling mechanism, and Thompson (1989), Fischer *et al.* (1992), Rowan & Kligfield (1992), and Holl & Anastasio (1993) provide evidence for fixing-hinge growth of folds that could be interpreted as detachment folds. We have observed multiple detachment folds whose distribution of strain indicates that hinges were fixed during most or all of folding (e.g. Homza 1993). An important implication of fixed-hinge fold growth is that fold limbs rotate during fold growth, as observed in many natural folds (e.g. Hardy & Poblet 1994), in contrast with the fixed limb orientations of ideal fault-bend or fault-propagation folds (Suppe 1983, Suppe & Medwedeff 1990, Mitra 1990).

Dahlstrom (1990) pointed out that fixed arc-length folding is incompatible with conservation of cross-sectional area for a constant detachment depth, which requires a linear relationship between shortening and uplifted cross-sectional area (equation 2) (Fig. 13). In contrast, Wiltschko & Chapple (1977) documented a non-linear relationship between uplifted area and shortening for symmetrical fixed arc-length folds (Figs. 8a, 9 and 13). The incompatibility between constant detachment depth and fixed arc-length folding is particularly obvious for fixed arc-length folds with interlimb angles less than a critical value, below which uplifted area decreases with increasing shortening (Wiltschko & Chapple 1977) (Fig. 13). Wiltschko & Chapple (1977) resolved this problem by assuming that incompetent material moves from synforms to antiforms as uplifted area initially increases, then flows out of the antiforms as area decreases with increasing shortening, resulting in a change in detachment depth with fold evolution. The present models quantitatively illustrate the fundamental incompatibility of the assumption of constant detachment depth with the growth of fixed arc-length folds. They show that detachment depth must change as a fixed arc-length fold evolves (Figs. 5b and 8), and allow the required changes in detachment depth to be determined (equation 19 and Figs. 8 and 9).

In order for a detachment fold to grow with a constant detachment depth, the uplifted area in its core must increase linearly as shortening increases (Fig. 13). This requires an increase in length of one or more fold limbs, which in turn requires hinge migration (Fig. 12b). Growth of folds by hinge migration has been documented for kink bands (Weiss 1968, Stewart & Alvarez 1991), and has been used to model fault-bend folds (Suppe 1983) and fault-propagation folds (Suppe & Medwedeff 1990). Dahlstrom (1990) and Butler (1992) concluded that hinge migration is likely during growth of detachment folds and some Alpine fold nappes, respectively. The geometric models of detachment folds of Jamison (1987) and Mitra & Namson (1989) both assume a fixed detachment depth and fold growth by hinge migration.

Thus, some evidence argues for fixed-hinge growth of detachment folds whereas geometric models assuming constant detachment depth require the growth of detachment folds by hinge migration. Whether any or all natural detachment folds grow with fixed hinges remains an important but unresolved question. Since our first model is based on the assumption of constant detachment depth, it requires hinge migration for the growth of detachment folds. However, the variable detachment depth model shows that fixed arc-length folds, as well as other folds with geologically reasonable kinematic paths that are incompatible with fixed-depth models, may evolve above a detachment unit that varies in thickness during deformation (Figs. 8 and 10b). The observation that detachment depth does in fact commonly vary in natural detachment folds (e.g. Wiltschko & Chapple 1977, Davis & Engelder 1985, Wallace 1993, Homza & Wallace unpublished field observations) suggests that the variable-depth model may have useful application to natural detachment folds.

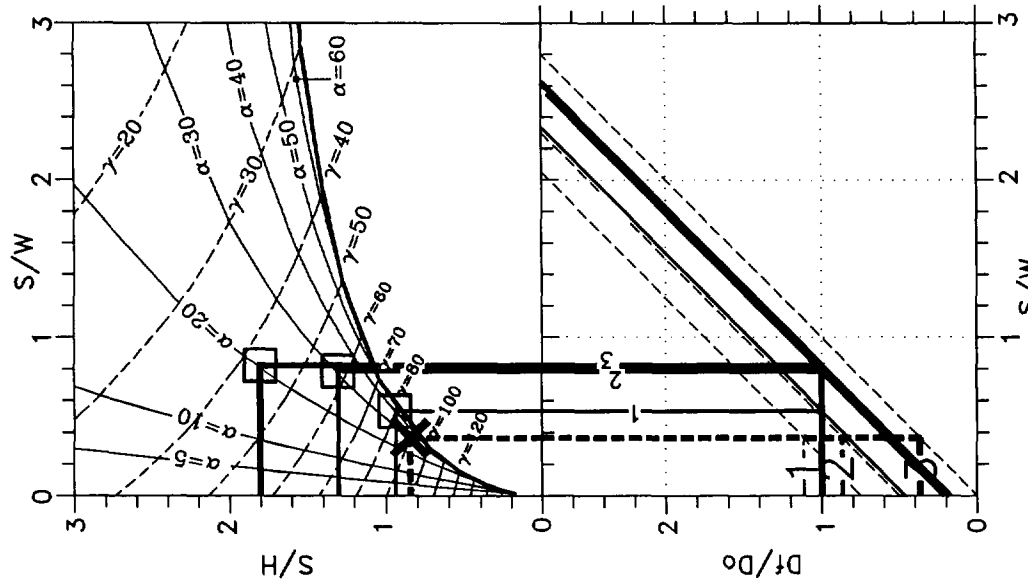

Fig. 11. Graphical plot of the two fold sequences in Fig. 10 on the variable-depth diagram. The line thicknesses and line-types correspond to the folds in Fig. 10. The plot of fold sequence 10(a) (□) shows α and γ decreasing while both S/H and S/W increase. The detachment depth is constant, so $Df/Do = 1$. The plot of fold sequence 8(b) (x) is a single point since the geometry is self-similar; detachment depth progressively decreases.

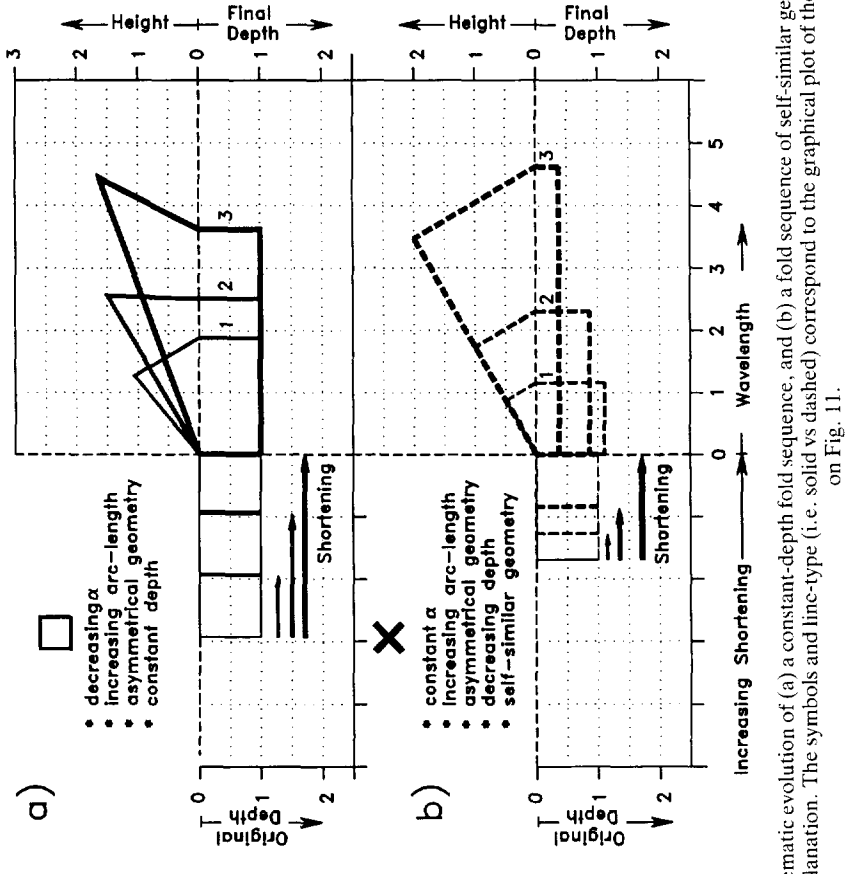

Fig. 10. Kinematic evolution of (a) a constant-depth fold sequence, and (b) a fold sequence of self-similar geometries. See Fig. 8 for explanation. The symbols and line-type (i.e. solid vs dashed) correspond to the graphical plot of these sequences on Fig. 11.

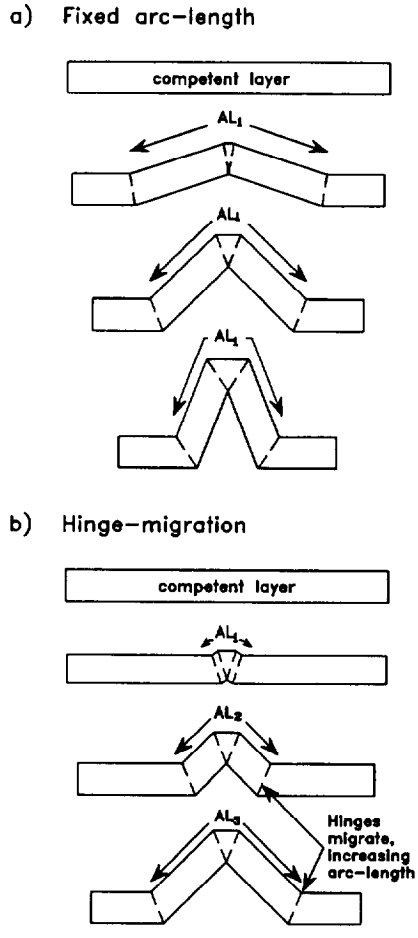

Fig. 12. Diagram showing the fundamental difference in kinematics between fixed arc-length folding (a), in which the arc-length remains constant and hinges are fixed throughout the evolution of the fold, and folding by hinge-migration (b), in which arc-length increases. AL = arc length.

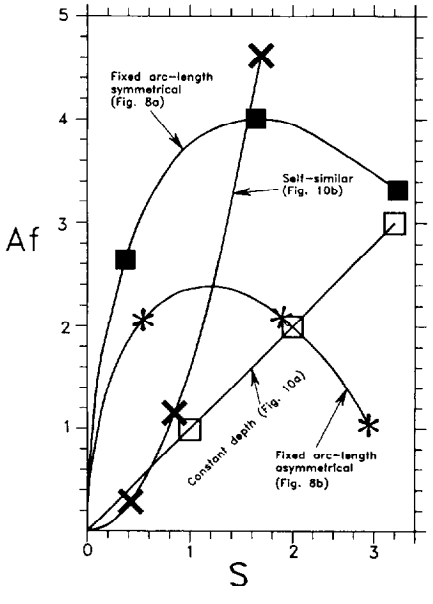

Fig. 13. Plot of shortening (S) vs uplifted cross-sectional area (A_f) for fold sequences in Figs. 8 and 10. Any fold sequence with a constant detachment depth D_c follows a straight line with slope D_c. Other fold sequences follow non-linear curves.

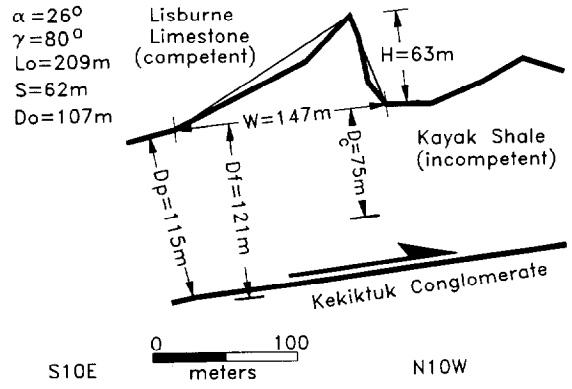

Fig. 14. Simplified cross-section of the Salisbury Creek anticline showing detachment depth solutions calculated using both the conventional equal-area technique (equation 2) and the variable-depth technique (equation 19). The fold axis is horizontal and the plane of section is vertical. Calculations use the enveloping surface shown. D_c = detachment depth calculated from equations (2) or (12), D_f = detachment depth calculated from equation (19), D_o = undeformed thickness of Kayak Shale determined from a panel of Lisburne Limestone that parallels the detachment surface. D_p = depth to detachment projected into the line of section. Other variables as illustrated in Figs. 2 and 6. The fold geometry is plotted on Fig. 7.

APPLICATION OF THE VARIABLE DETACHMENT DEPTH METHOD TO A NATURAL DETACHMENT FOLD

The Salisbury Creek anticline in the northeastern Brooks Range of Alaska is defined by several hundred meters of the competent Mississippian to Pennsylvanian Lisburne Limestone and is cored by the internally deformed, incompetent Mississippian Kayak Shale (Fig. 14). Stratigraphically beneath the Kayak Shale, the Mississippian Kekiktuk Conglomerate is deformed in folds with much longer wavelength and larger interlimb angle, requiring a detachment to exist in the Kayak Shale (Namson & Wallace 1986, Wallace & Hanks 1990, Homza 1993, Wallace 1993).

If constant line-length, plane strain, and chevron geometry (shown as an enveloping surface on Fig. 14) are assumed, then the geometry of the Salisbury Creek anticline requires 62 m of shortening (the fold is plotted on Fig. 7). If constant detachment depth is also assumed, then equations (3) and (12) require a detachment depth (D_c) of 75 m (Fig. 14). If constant depth is not assumed and the undeformed thickness (D_o) of the Kayak Shale is used in equation (19), then the final thickness (D_f) required for the fold to balance is 121 m. The observed detachment surface projects into the plane of section at 115 m (D_p) beneath the southern syncline, and thus agrees well with the depth calculated if constant detachment depth is not assumed.

Since the variable detachment depth method incorporates an additional observational constraint, the undeformed thickness (D_o), it is less sensitive to observational uncertainties than is the constant depth method. For example, if the detailed geometry of the Salisbury Creek anticline, where $S = 65$ m and $A_f = 3809$ m^2, is used in the calculations instead of the triangular enveloping surface, then $D_c = 59$ m and $D_f = 128$ m.

Thus, using the enveloping surface as an approximation creates an error of 16 m in the constant-depth calculation, but it creates an error of only 7 m in the variable-depth calculation. This difference in sensitivity holds true for other variables as well.

Since the variable-depth solution incorporates the additional data (D_o) and more closely matches the projected depth, it is considered more reasonable than the constant-depth solution. Hence, the kinematic path followed by the Salisbury Creek anticline is not restricted by the requirement of constant detachment depth and could have evolved geometrically by either fixed- or migrating-hinge kinematics. The area observed beneath the fold ($W \times D_p = 147\text{ m} \times 115\text{ m} = 16{,}905\text{ m}^2$) is less than the area calculated using the variable-depth model ($W \times D_f = 147\text{ m} \times 128\text{ m} = 18{,}816\text{ m}^2$) by ~ 1911 m^2. This discrepancy suggests that a significant amount of incompetent rock could have been removed from the fold. Strong solution cleavage and stylolitization in the Kayak Shale in the core of the anticline support this suggestion.

Shortening (thickening) of the incompetent unit outside of the fold presumably is accommodated in the competent unit by folding, which would also result in an overestimate of thickening below the fold using the variable-depth model. However, thickening in the incompetent unit outside of the fold is not accounted for by the variable-depth model, since an assumption of the model is that no incompetent material flows through the synclinal hinges bounding the detachment fold. The difficulty in determining the distance over which fold shortening has influenced incompetent unit thickness and how changes in incompetent unit thickness are partitioned between adjacent folds is a fundamental problem with this or any geometric model for detachment folds.

Qualitative analysis of the distribution of strain in the Salisbury Creek anticline provides constraints on its kinematic evolution. The anticlinal hinge is extremely strained and includes many minor contractional faults with a variety of orientations and offsets, abundant centimeter-scale folds, well-developed calcite-filled veins that parallel and cross-cut bedding, tectonic brecciation, solution cleavage, and stylolitization. The synclines bounding the forelimb and the backlimb are similarly very strained. Little solution cleavage and only very minor stylolitization are apparent in the backlimb. Centimeter-thick chert beds at the base of the Lisburne Limestone record only a few poorly developed veins and no tectonic brecciation in the backlimb. The only significant deformation in the backlimb is recorded by bed-parallel slickensides indicating flexural slip and a late-stage thrust fault with about 10 m of displacement. Forelimb deformation includes tectonically brecciated and boundinaged chert beds, minor cleavage, bed-parallel veins of stretched calcite fibers, and stretched bed-parallel slickenfibers indicating north-over-south flexural slip.

There are no structures reflecting hinge migration through the backlimb, nor are there any definitive examples of such structures in the forelimb. The intensity of tectonic brecciation and interbed shear in the forelimb permits the possibility that either adjacent hinge migrated through the forelimb during the early stages of fold growth. However, we prefer a fixed-hinge interpretation because the contractional faults, cross-cutting veins, minor folds and intense solution cleavage that characterize the adjacent fold hinges are lacking in the forelimb. Consequently, we suggest that the Salisbury Creek anticline formed by fixed-hinge buckling, with structural thickening of the Kayak Shale, volume loss in the Kayak Shale due to fluid migration out of the core of the fold, and late-stage thrust faulting in the backlimb.

DISCUSSION

Incorporation of different assumptions into the variable-depth model

The example illustrates that the variable-depth model can be applied successfully to a natural detachment fold and, at least for that fold, yields a better approximation than the constant-depth model. A variety of modifications can be made to the variable-depth model to accommodate departures of natural folds from the assumptions incorporated in the model. For instance, the example illustrates a problem with the assumption of constant cross-sectional area of the incompetent unit within the synforms bounding the fold. In its present form, the model does not account for changes in cross-sectional area of the incompetent unit due to flow through synformal hinges, loss or gain of rock volume, and/or transport of rock into or out of the plane of section. The effect of observed area changes can easily be accommodated in the model by making appropriate corrections to the area differential ($A_{\Delta D}$), provided that the area changes affect only the incompetent unit and do so uniformly. Applying such corrections will yield a corrected value of the change in thickness (ΔD), although determining accurate values of corrections for natural folds may be difficult in practice. The need for corrections is eliminated if both original (D_o) and final (D_f) detachment depth are known, allowing the change in thickness (ΔD), and consequent loss or gain of area, to be determined directly. Non-uniform changes in the area of the incompetent unit and uniform or non-uniform changes in the length of the competent unit would necessitate more complicated corrections, requiring a detailed knowledge of the amount, distribution, and timing (relative to folding) of any area or length changes.

Although only simple triangular fold geometries are considered in the model, the same approach could be applied to other fold geometries, although the complexity of the problem will increase as the number of possible hinges is increased and if non-linear limbs are considered. The model could be modified to accommodate vertical differences in layer-parallel shear in the

Table 1. Table comparing the geometric and kinematic characteristics of ideal fault-bend folds, fault-propagation folds, and detachment folds with fixed or migrating hinges

	Fault-bend fold (1,2)	Fault-propagation fold (1,3)	Detachment fold (migrating hinges) (1,4)	Detachment fold (fixed hinges) (4)
Mechanical stratigraphy	Competent	Competent	Competent over incompetent	Competent over incompetent
Rigid footwall ramp	Yes	Yes	No	No
Detachment depth	Constant	Constant	Constant *or* variable (Thickness of incompetent unit below regional datum)	Variable
Fixed vs migrating hinges	Fixed in HW ramp Migrating over FW ramp	Migrating except in anticlinal core	Migrating	Fixed
Fixed vs rotating limbs	Fixed	Fixed	Fixed or rotating	Rotating
Forelimb dip	0–60° (I), 60–180° (II)*	0–180°	0–180°	0–180°
Backlimb dip	0–30°	0–60°	0–180°	0–180°
Kinematic paths				
Arc length	Increasing	Increasing	Increasing†	Fixed
Wavelength	Increasing	Increasing	Increasing *or* decreasing†	Decreasing
Height	Increasing to a maximum	Increasing	Increasing *or* Increasing then decreasing†	Increasing then decreasing

References: (1) Jamison (1987), (2) Suppe (1983), (3) Suppe & Medwedeff (1990), (4) this paper.
Notes: Constant bed thickness (parallel folding) assumed in competent units.
Ramp assumed to step up from bed-parallel detachment (décollement) for FBF and FPF.
*(I): mode I FBF's, (II): mode II FBF's.
†Geometrically unconstrained; the most geologically plausible paths are noted.

incompetent unit by using the shear profile to define the trailing surface of the deformed area of the incompetent unit. This would enable a correct change in thickness (ΔD) to be determined, rather than the incorrect value that would be determined if the shortening value indicated by the fold shape was used assuming no vertical differences in layer parallel shear in the incompetent unit. The model is not affected by vertical variations in layer-parallel shear in the competent unit since it addresses only the geometry of the interface between the competent and incompetent units.

Comparison of ideal detachment folds with ideal fault-bend and fault-propagation folds

Our models provide a quantitative basis for the conclusion that ideal detachment folds are intrinsically less constrained, and hence less predictable, than ideal fault-bend or fault-propagation folds (Fig. 1). Similar relationships among fold geometry (width, height, backlimb dip, forelimb dip), shortening and detachment depth can be established for all three fold types. However, a greater range of geometries for detachment folds is possible within the common assumptions of plane strain and constant cross-sectional area, detachment depth and competent bed length and thickness (Jamison 1987) (Table 1). This reflects the fact that both backlimb and forelimb dip are dependent on ramp angle in ideal fault-bend and fault-propagation folds (Suppe 1983, Suppe & Medwedeff 1990, Mitra 1990, Jamison 1987), whereas the mobility of the incompetent unit in detachment folds requires no such linkage between backlimb and forelimb dip. If the assumption of constant detachment depth is relaxed for detachment folds, as in our variable-depth model, an even wider range of values of original and final detachment depth are possible for each fold geometry.

The contrast is even more apparent in the kinematic evolution of ideal fault-bend and fault-propagation folds vs that of ideal detachment folds (Table 1). Detachment depth and interlimb angle are fixed during growth of ideal fault-bend and fault-propagation folds as long as it is assumed that bed thickness remains constant and no vertical gradient exists in layer-parallel shear (Suppe 1983, Suppe & Medwedeff 1990, Mitra 1990, 1992, Jamison 1987). These constraints exist because the ideal fold geometry is controlled by fixed, competent footwall ramps. The mobility of the incompetent unit in an ideal detachment fold allows a fundamentally different kinematic evolution from these 'rigid-ramp' folds. Variation of backlimb and/or forelimb dip is geometrically possible with the constant-depth model (Fig. 4), allowing a wider variety of kinematic paths, yet self-similar (fixed backlimb and forelimb dip) fold growth is not (Fig. 5a). If the assumption of constant detachment depth is relaxed for detachment folds, as in our variable-depth model, an even wider array of kinematic paths is possible, including fixed-hinge (Fig. 8) and self-similar (Fig. 10b) fold growth, as well as a variety of paths that are geometrically possible but not kinematically or mechanically plausible.

Fixed, competent footwall ramps account for migrating hinges in the hangingwalls of ideal fault-bend and fault-propagation folds (Table 1). However, there is no rigid 'footwall' topography in a detachment fold, thereby precluding the geometric requirement of mi-

grating hinges. In fact, the inherent mobility of the incompetent unit in detachment folds suggests that a focus on the geometry of the competent unit may be the best approach to constraining the possible geometries and kinematic paths of detachment folds. Given the observational and theoretical evidence in support of fixed-hinge growth of buckle folds, it may well be that fixed hinges in the competent unit are the dominant control on the geometry and kinematic evolution of detachment folds. Under the assumptions of our models, such growth is possible only if incompetent unit thickness, and hence detachment depth, varies.

Applicability of our models to natural detachment folds

Our geometric models, in and of themselves, do not indicate the behavior of natural detachment folds. However, they do provide a simple, mathematically constrained basis to explore what is geometrically and kinematically possible given a well-defined set of starting assumptions. These conceptual models can be tested against natural detachment folds with well-constrained geometry and/or kinematic evolution in order to determine which assumptions are valid for those folds, hopefully leading to some general insights into the geometry and kinematics of natural detachment folds. However, the range of variability that the models demonstrate to be possible, coupled with the likelihood that some of the assumptions are not appropriate for natural detachment folds, indicates that caution should be used in applying these—or any other—simple, geometric models to the reconstruction of natural detachment folds whose geometry is not fully constrained by data. Specifically, a unique solution for detachment depth from fold geometry alone is possible only if constant detachment depth is assumed, and this assumption has been shown to be invalid for at least some natural detachment folds. While the variable-depth model allows determination of either original or final detachment depth if the other is known, it is only an approximation because it requires the geologically unreasonable assumption that no incompetent material is transported through the bounding synformal hinges of a detachment fold.

The same basic technique upon which our models are based, line-length balancing of the competent unit and area balancing of the incompetent unit, can overcome some of the limitations of the geometric models if it is applied over a large enough area to account for complex flow of the incompetent unit. Specifically, balancing along a long enough line of section may account for flow through synclinal hinges and balancing of multiple sections along strike may account for flow transverse to the line of section. Careful observations of mesoscopic and microscopic structures and strain measurements may be needed to validate model assumptions and to correct for departures from those assumptions. These certainly are not new insights, and are routinely addressed in discussions of cross-section balancing (e.g. Woodward *et al.* 1985, 1989). However, by demonstrating the sheer variability in possible detachment folds, our models illustrate the limits of simple geometric models in reconstructing detachment folds whose geometry and detachment depth are not fully constrained, particularly if it is not assumed that detachment depth remains constant. These points emphasize the importance of using additional approaches in reconstructing detachment fold geometry, rather than relying on simple geometric models as heavily as may be possible with geometrically more constrained folds, such as fault-bend or fault-propagation folds.

CONCLUSIONS

We have presented two conceptual geometric models for idealized detachment folds that provide strict quantitative constraints on the fold geometry and kinematics possible given an explicit set of starting assumptions. The constant detachment depth model shows that growth of a detachment fold with constant detachment depth requires a linear increase in area with increasing shortening. This, in turn, precludes fixed-hinge (fixed arc-length) and self-similar (fixed limb-dip) fold growth, both of which require non-linear changes of area with increasing shortening. Fold growth along these kinematic paths, as well as others that are precluded by the constant detachment depth model, is possible if the assumption of constant detachment depth is relaxed, as in the variable detachment depth model. Both models require detachment folds to nucleate with symmetrical geometries or very high ratios of wavelength to height.

Variable detachment depth, as determined by incompetent unit thickness in synforms, has been observed in natural detachment folds, and fixed-hinge growth of buckle folds is supported by observational and theoretical evidence. Together, these suggest that the variable-depth model is a better approximation for many natural detachment folds than any constant-depth model.

The mobility of the incompetent unit in detachment folds makes these folds intrinsically less constrained than ideal fault-bend and fault-propagation folds, which have rigid footwall ramps. This intrinsic variability limits the usefulness of simple geometric models for reconstructing the geometry of natural detachment folds. This reinforces the importance of balancing over a sufficiently large area, across and along structural strike, to account for variations in detachment depth and of evaluating strain to correct model assumptions. However, as has been shown here, geometric models are very useful to assess the geometric and kinematic implications of specific assumptions, and can serve as a basis for testing the validity of those assumptions for natural detachment folds whose geometry is well constrained.

Acknowledgements—This paper is based in part on Master's and Ph.D. studies by Homza, supervised by Wallace. The project was supported by NSF grant EAR-9304482, grants to the Tectonics and Sedimentation Research Group at the University of Alaska from Amoco, ARCO, BP (Alaska), Chevron, Conoco, Elf, Exxon, Japan National Oil Corp., Mobil, Murphy, Phillips, Shell, Texaco, and Unocal, and to Homza from the Graduate Resource Fellowship, Geist Fund, and Austin Cooley Fund of the University of Alaska Fairbanks.

We thank S. Wojtal and the anonymous reviewers of earlier versions of this manuscript and related proposals for their helpful comments.

REFERENCES

Abbassi, M. R. & Mancktelow, N. S. 1992. Single layer buckle folding in non-linear materials—I, experimental study of development from an isolated initial perturbation. *J. Struct. Geol.* **14**, 85–104.

Biot, M. A. 1961. Theory of folding of stratified viscoelastic media and its implication in tectonics and orogenesis. *Bull. geol. Soc. Am.* **72**, 1595–1620.

Bucher, W. H. 1933. *Deformation of the Earth's Crust*. University Press, Princeton, New Jersey.

Butler, R. W. H. 1992. Evolution of Alpine fold-thrust complexes: a linked kinematic approach. In: *Structural Geology of Fold and Thrust Belts* (edited by Mitra, S. & Fisher, G. W.). The Johns Hopkins University Press, Baltimore, 29–44.

Chamberlin, R. T. 1910. The Appalachian folds of central Pennsylvania. *J. Geol.* **18**, 228–251.

Currie, J. B., Patnode, H. W. & Trump, R. P. 1962. Development of folds in sedimentary strata. *Bull. geol. Soc. Am.* **73**, 655–674.

Dahlstrom, C. D. A. 1969. The upper detachment in concentric folding. *Bull. Can. Petrol. Geol.* **17**, 326–346.

Dahlstrom, C. D. A. 1970. Structural geology in the eastern margin of the Canadian Rocky Mountains. *Bull. Can. Petrol. Geol.* **18**, 322–406.

Dahlstrom, C. D. A. 1990. Geometric constraints derived from the law of conservation of volume and applied to evolutionary models for detachment folding. *Bull. Am. Ass. Petrol. Geol.* **74**, 336–344.

Davis, D. M. & Engelder, T. 1985. The role of salt in fold-and-thrust belts. *Tectonophysics* **119**, 67–88.

de Sitter, L. U. 1956. *Structural Geology*. McGraw Hill, New York.

Dixon, J. M. & Liu, S. 1992. Centrifuge modelling of the propagation of thrust faults. In: *Thrust Tectonics* (edited by McClay, K. R.). Chapman and Hall, London, 53–70.

Dixon, J. M. & Tirrul, R. 1991. Centrifuge modelling of fold-thrust structures in a tripartite stratigraphic succession. *J. Struct. Geol.* **13**, 3–20.

Epard, J. L. & Groshong, R. H. 1993. Excess area and depth to detachment. *Bull. Am. Ass. Petrol. Geol.* **77**, 1291–1302.

Fischer, M. P., Woodward, N. B. & Mitchell, M. M. 1992. The kinematics of break-thrust folds. *J. Struct. Geol.* **14**, 451–460.

Geiser, P. A. 1988. The role of kinematics in the construction and analysis of geologic cross-sections in deformed terranes. In: *Geometries and Mechanisms of Thrusting, with Special Reference to the Appalachians* (edited by Mitra, G. & Wojtal, S.). *Spec. Pap. geol. Soc. Am.* **222**, 47–76.

Goguel, J. 1962. *Tectonics*. Freeman, San Francisco.

Hardy, S. & Poblet, J. 1994. Geometric and numerical model of progressive limb rotation in detachment folds. *Geology* **22**, 371–374.

Holl, J. E. & Anastasio, D. J. 1993. Paleomagnetically derived folding rates, southern Pyrenees, Spain. *Geology* **21**, 271–274.

Homza, T. X. 1992. A detachment fold-truncation duplex southwest of Bathtub Ridge–northeastern Brooks Range, Alaska. Unpublished M.S. thesis, University of Alaska, Fairbanks.

Homza, T. X. 1993. Preliminary observations of the Straight Creek detachment anticline–northeastern Brooks Range, Alaska: a basis for geometric and kinematic detachment fold models. *Alaska Div. Geol. and Geophys. Surv. Public Data File*, 93-43.

Hossack, J. R. 1979. The use of balanced cross-sections in the calculation of orogenic contraction: A review. *J. geol. Soc. Lond.* **136**, 705–711.

Jamison, W. R. 1987. Geometric analysis of fold development in overthrust terranes. *J. Struct. Geol.* **9**, 207–219.

Johnson, A. M. 1977. *Styles of Folding*. Elsevier, Amsterdam.

Laubscher, H. P. 1962. Die Zweiphasenhypothese der Jurafaltung. *Eclog. geol. Helv.* **55**, 1–22.

Mancktelow, N. S. & Abbassi, M. R. 1992. Single layer buckle folding in non-linear materials—II, comparison between theory and experiment. *J. Struct. Geol.* **14**, 105–120.

Mitchell, M. M. & Woodward, N. B. 1988. Kink detachment fold in the southwestern Montana fold and thrust belt. *Geology* **16**, 162–165.

Mitra, S. 1990. Fault-propagation folds: geometry, kinematic evolution, and hydrocarbon traps. *Bull. Am. Ass. Petrol. Geol.* **74**, 921–945.

Mitra, S. 1992. Balanced structural interpretations in fold and thrust belts. In: *Structural Geology of Fold and Thrust Belts* (edited by Mitra, S. & Fisher, G. W.). The Johns Hopkins University Press, Baltimore,53–77.

Mitra, S. & Namson, J. S. 1989. Equal-area balancing. *Am. J. Sci.* **289**, 563–599.

Namson, J. S. & Wallace, W. K. 1986. A structural transect across the northeastern Brooks Range, Alaska. *Geol. Soc. Am. Abstr. w Prog.* **18**, 163.

Ramberg, H. 1964. Selective buckling of composite layers with contrasted rheological properties, a theory for simultaneous formation of several orders of folds. *Tectonophysics* **1**, 307–341.

Ramsay, J. G. 1967. *Folding and Fracturing of Rocks*. McGraw Hill, New York.

Ramsay, J. G. 1974. Development of chevron folds. *Bull. geol. Soc. Am.* **85**, 1741–1754.

Rowan, M. G. & Kligfield, R. 1992. Kinematics of large-scale asymmetric buckle folds in overthrust shear: an example from the Helvetic nappes. In: *Thrust Tectonics* (edited by McClay, K. R.). Chapman and Hall, London, 165–173.

Stewart, K. G. & Alvarez, W. 1991. Mobile-hinge kinking in layered rocks and models. *J. Struct. Geol.* **13**, 243–259.

Suppe, J. 1983. Geometry and kinematics of fault-bend folding. *Am. J. Sci.* **283**, 684–721.

Suppe, J. & Medwedeff, D. A. 1990. Geometry and kinematics of fault-propagation folding. *Eclog. geol. Helv.* **83**, 409–454.

Thompson, R. I. 1989. Stratigraphy, tectonic evolution and structural analysis of the Halfway River map area (94 B), northern Rocky Mountains, British Columbia. *Mem. Geol. Surv. Can.* **425**.

Wallace, W. K. 1993. Detachment folds and a passive-roof duplex: Examples from the northeastern Brooks Range, Alaska. In: *Short Notes on Alaskan Geology* 1993 (edited by Solie, D. N. & Tannian, F.). *Alaska Div. Geol. & Geophys. Surv. Professional Report* **113**, 81–99.

Wallace, W. K. & Hanks, C. L. 1990. Structural provinces of the northeastern Brooks Range, Arctic National Wildlife Refuge, Alaska. *Bull. Am. Ass. Petrol. Geol.* **74**, 1100–1118.

Weiss, L. E. 1968. Flexural slip folding of foliated model materials. In: *Kink Bands and Brittle Deformation* (edited by Baer, A. J. & Norris, D. K.). *Geol. Surv. Pap. Can.* **68**, 294–357.

Willis, B. & Willis, R. 1934. *Geologic Structures*. McGraw Hill, New York.

Wiltschko, D. V. & Chapple, W. M. 1977. Flow of weak rocks in the Appalachian Plateau folds. *Bull. Am. Ass. Petrol. Geol.* **61**, 653–670.

Woodward, N. B., Boyer, S. E. & Suppe, J. 1985. An outline of balanced cross-sections. Univ. of Tennessee, Studies in Geology **11**, 2nd edition.

Woodward, N. B., Boyer, S. E. & Suppe, J. 1989. Balanced geological cross-sections: An essential technique in geological research and exploration. *American Geophysical Union Short Course in Geology* **6**.